Desalination and Water Treatment
www.deswater.com

doi: 10.5004/dwt.2020.25618

189 (2020) 316–328
June

Facile synthesis of magnetic $MnFe_2O_4$/Mg-Al hydrotalcite composites for phosphate removal

Weida Wang[a,†], Yiming Qin[a,†], Weiping Li[a,*], Tingting Zhang[a,b], Xin Chang[a]

[a]*School of Energy and Environment, Inner Mongolia University of Science and Technology, Baotou 014010, Inner Mongolia, China, Tel. +86 04725953154; emails: sjlwp@163 (W. Li), wangweida888@163.com (W. Wang), 2226883525@qq.com (Y. Qin), zhangtingkl1314@163.com (T. Zhang), 1804779124@qq.com (Chang)*
[b]*School of Environment and Municipal Engineering, Xi'an University of Architecture and Technology, Xi'an 710055, Shaanxi, China*

Received 19 June 2019; 25 January 2020

ABSTRACT

Magnetic manganese ferrites/magnesium-aluminum hydrotalcite composites ($MnFe_2O_4$/MgAl-LDO) were prepared by the facile coprecipitation method and were characterized by scanning electron microscope, energy dispersive spectrometer, X-ray Diffraction, Fourier transform infrared spectroscopy, and vibrating sample magnetometer. The influence factors such as initial pH, a dosage of $MnFe_2O_4$/MgAl-LDO, reaction time, temperature, and initial concentration of phosphate solution have evaluated through batch experiments. The adsorption characteristics were analyzed by kinetics and adsorption thermodynamics models. The results showed that the adsorption of phosphate from an aqueous solution by $MnFe_2O_4$/MgAl-LDO was influenced by the factors that had tested markedly. The optimum pH for the adsorption of phosphorus was 4.0, the optimum adsorption dosage was 3 g/L, the appropriate reaction temperature was 30°C, and the optimum phosphate concentration was 2 mg/L. Adsorption kinetics fitting results indicated that the pseudo-second-order model was appropriate for describing the sorption process. The adsorption isotherm coincided well with the Langmuir isothermal adsorption model. The parameters of the adsorption thermodynamics were $\Delta G < 0$ and $\Delta H > 0$ showed that the process of phosphate adsorption by $MnFe_2O_4$/MgAl-LDO was spontaneous and endothermic.

Keywords: Magnetic $MnFe_2O_4$; MgAl-LDO; Phosphate; Adsorption

1. Introduction

The eutrophication of freshwater lakes has become a global water pollution problem, and it has attracted widespread attention recently. In 2016, eutrophic lakes accounted for about 87.6% of all the lakes in China [1,2]. Phosphorus is one of the key factors responsible for eutrophication, and it is also an indispensable primary substance for the growth of phytoplankton. Algae can survive and reproduce in large quantities depending on the quantity of organic compounds containing phosphorus in water [3]. The existence of multitudinous algae could reduce the dissolved oxygen content in water, leading to a deterioration of its quality. The occurrence of harmful algal bloom and other lake eutrophication pollution events threaten the hydro-ecological health, or even the health of humans, who use this water for drinking purposes [4]. Therefore, it is crucial to monitor and reduce the content of phosphorus in water for the protection and control of water ecology.

At present, various methods such as chemical precipitation, biological treatment, electrochemical method, and adsorption have been developed for removing phosphorus from wastewater. Among these techniques, adsorption has attracted extensive attention in wastewater treatment in

* Corresponding author.

† These authors have contributed equally to this article.

recent years due to its advantages such as simple process, stable operation, low-cost, and no secondary pollution [5]. Numerous adsorbents have been developed for water treatment, such as zeolite, attapulgite, bentonite, and so on [6–8]. Layered double hydroxides (LDHs), also known as bimetallic hydroxides, are a typical layered functional material that belongs to the class of hexagonal systems, and its structure is similar to that of clay minerals, with a lamellar structure of brucite [9]. It is an inorganic anion exchanger with a large specific surface area, high anion exchange capacity, structure memory effect, and interlayer anion exchangeability for removing pollution from wastewater [10]. Substantial amounts of carbonate and water molecules are present in hydrotalcite, and the carbonate can be converted into carbon dioxide, which escapes from the interlayer with water molecules when the hydrotalcite was calcinated at a high temperature. The space left by the carbonate could be a possible zone for the introduction of metals and inorganic ions. The process of calcination and adsorption can be described as follows [11]:

$$Mg_{1-x}^{2+}Al_x^{3+}(OH)_2(CO_3)_{x/2}\times m\,H_2O \xrightarrow{450^{\circ}C} Mg_{1-x}^{2+}Al_x^{3+}O_{1+x/2} + x/2\,CO_2 + (m+1)\,H_2O \quad (1)$$

$$Mg_{1-x}^{2+}Al_x^{3+}\,O_{1+x/2} + x/nA^{n-} + (m+1+x/2)\,H_2O \rightarrow Mg_{1-x}^{2+}Al_x^{3+}(OH)_2\,A_{x/n}\times m\,H_2O + OH^- \quad (2)$$

Mg/Al-LDH effectively adsorbs Cr(VI), and its adsorption capacity is 105.15 mg/g. A lower pH is beneficial to the completion of the adsorption process, and its adsorption capacity for methyl orange is 1,219.5 mg/g, which indicates a significant adsorption capacity for organic matter [12,13]. This layered material also has an adsorption effect on anions such as F^-. It is capable of performing adsorption at different values of pH, and its maximum adsorption capacity is 2.5 mg/g [14]. LDH has been widely applied for the removal of metal ions and organic dyes due to its excellent adsorption properties. However, LDH is difficult to separate and recover when its adsorption capacity reaches saturation.

In recent years, magnetic separation technology has been developed and applied in the adsorption realm because of its ability to be easily separated with an external magnetic field and large specific surface area of magnetic particles such as Fe_2O_3, Fe_3O_4, and $CoFe_2O_4$. Owing to its characteristics such as convenient preparation, excellent chemical stability, fine saturation magnetization, and large specific surface area, magnetic manganese ferrite particles ($MnFe_2O_4$) have been applied for contaminant adsorption [15,16]. Yi et al. [17] studied the adsorption of Cr(VI) by $MnFe_2O_4$, and the saturated adsorption capacity was found to be 7.325 mg/g. Furthermore, $MnFe_2O_4$ has been applied for the adsorption of organic compounds such as methylene blue. Its adsorption capacity was found to be 29.94 mg/g when the pH was 9 [18]. However, studies on the adsorption properties of phosphorus by manganese ferrite and magnesium-aluminum hydrotalcite composite adsorbents are still rare. The combination of $MnFe_2O_4$ and LDO enables incorporating the advantages of both the excellent adsorption properties of hydrotalcite and the magnetic separation properties of manganese ferrite. This paper attempts to provide a reference for its practical application through the combination of the two materials.

In this study, magnetic manganese ferrites/magnesium-aluminum hydrotalcite ($MnFe_2O_4$/MgAl-LDO), an efficient magnetic adsorbents, were synthesized using the coprecipitation method and were employed for the removal of phosphate from an aqueous solution. The adsorption parameters such as the pH of the initial solution, adsorbent dosage, reaction time, and coexistence ion were studied through batch experiments. The fitting results of the adsorption kinetics, adsorption isotherm, and adsorption thermodynamics were used to explicate the adsorption mechanism. Experiments on the desorption and cyclic adsorption times were conducted to evaluate its repeatability and practicality.

2. Materials and methods

2.1. Materials

The guaranteed reagent KH_2PO_4 was used in this study and it was purchased from Shanghai Maikelin Biochemical Technology Co. Ltd., China. The other analytical reagents, $FeCl_3{\cdot}6H_2O$, $MnSO_4{\cdot}H_2O$, $Mg(NO_3)_2{\cdot}6H_2O$, and $Al(NO_3)_3{\cdot}9H_2O$, were purchased from Feng Chuan Chemical Reagent Technology Co. Ltd., China. The conditional pH of the phosphate solution was adjusted by varying concentrations of HCl and NaOH solutions. Also, deionized water was used in this experiment.

The coprecipitation method was adopted for the synthesis of the magnetic $MnFe_2O_4$ particles: 8.1 g of $FeCl_3{\cdot}6H_2O$ and 2.5 g of $MnSO_4{\cdot}H_2O$ were dissolved in 300 mL deionized water, followed by the addition of 10 mol/L NaOH solution drop by drop to obtain an alkaline solution of pH 10. Then, the beaker containing the solution was stirred at 80°C in a water bath for 8 h to obtain a uniform mixture. Subsequently, the solution was aged overnight in an oven at 60°C and cooled to room temperature after that. Magnetic $MnFe_2O_4$ was obtained as a precipitate in the lower layer. The beaker containing the $MnFe_2O_4$ was stirred by magnetic force at an appropriate speed to obtain an evenly distributed system. Then, a solution of $Mg(NO_3)_2{\cdot}6H_2O$ and $Al(NO_3)_3{\cdot}9H_2O$ with a molar ratio of 2:1 was added into the beaker by a peristaltic pump. A certain proportion of sodium hydroxide and sodium carbonate were added drop by drop into the solution to ensure that the pH was approximately 10. After this addition of magnesium and aluminum ions, the beaker was stirred for 2 h to ensure that the reaction was complete. The beaker was then aged for 8 h at 60°C in a blast oven, and the lower colloid was $MnFe_2O_4$/MgAl-LDH. The prepared adsorbent was collected using a vacuum suction pump. It was washed with deionized water to neutralize its pH and then dried in an oven. The adsorbent precursor was calcined in a muffle furnace at 450°C for 4 h. The magnetic adsorbent ($MnFe_2O_4$/MgAl-LDO) was then prepared after these procedures. Fig. 1 shows the flow chart of the preparation process.

2.3. Characterization

The morphology of the surface microstructures was characterized by scanning electron microscopy, energy

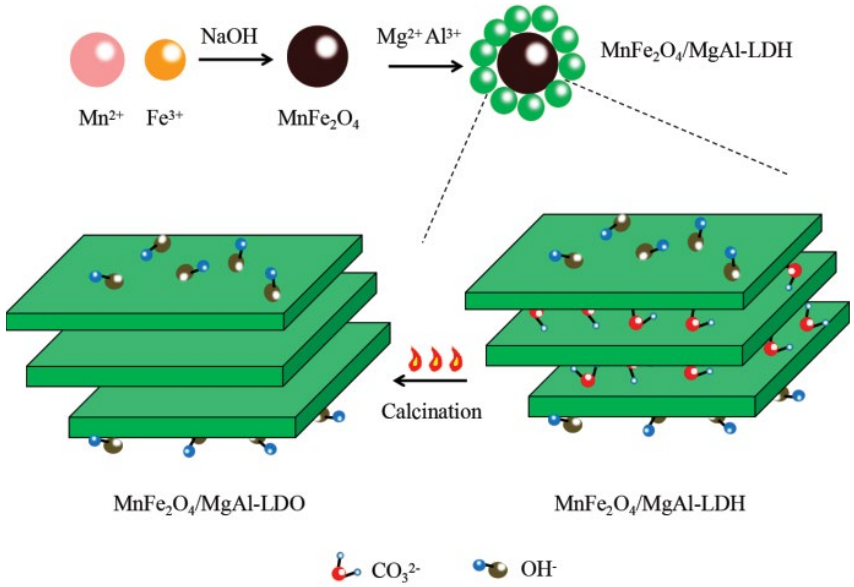

Fig. 1. Preparation and microstructure of magnetic $MnFe_2O_4$/MgAl-LDO.

dispersive spectroscopy (SEM-EDS, Quanta 400, USA), and transmission electron microscopy (TEM, Jeol 2100F, Japan Electronics Corporation). X-ray diffraction (XRD) was used to detect the elemental composition and crystal structure of the adsorbent (Escalab 250xi, Thermo Fisher, USA). The test range was from 10° to 80°, and the testing speed was 4° per minute. Fourier Transform Infrared Spectroscopy (FTIR) was employed to investigate the functional groups of the surface of the adsorbent, and the test range was 400–4,000 cm^{-1} (RX1, Perkin, USA). The magnetic properties of the adsorbents were measured using a vibrating sample magnetometer (VSM) (Quantum Design, MPMS-XL-7, USA).

2.4. Adsorption experiments

A certain amount of $MnFe_2O_4$/MgAl-LDO was added into 20 mL KH_2PO_4 solution with different concentrations. The pH of the initial solution was regulated by varying the concentrations of NaOH and HCl solutions (1 and 0.1 mol/L, respectively). The conical bottles with phosphate solution and adsorbent were placed in a constant temperature shaker and shaken at a rotation rate of 170 r/min until the adsorption reached its equilibrium state. Adsorption isotherm experiments were performed at three temperatures, namely 20°C, 30°C, and 40°C. Also, four kinds of solutions containing various concentrations of anions, CO_3^{2-}, SO_4^{2-}, Cl^-, and NO_3^- were employed for the competitive adsorption experiment. After that, the mixture solution was filtered by a 0.45 μm filter membrane. The residual phosphorus concentration of the adsorbed KH_2PO_4 solution was determined by an ultraviolet-visible spectrophotometer at λ = 700 nm. Parallel samples were obtained in all batch experiments. The phosphate removal rate and adsorption capacity were calculated by the following Eqs. (3) and (4):

$$R = \frac{C_0 - C_e}{C_e} \times 100\% \quad (3)$$

$$q_e = \frac{(C_0 - C_e) \times V}{m} \times 100\% \quad (4)$$

where R(%) is the removal rate of phosphate, C_0, and C_e (mg/L) are the phosphate concentrations at the initial stage and equilibrium time (min), respectively, q_e (mg/g) is the phosphate adsorption capacity, m (g) is the dosage of the adsorbent, and V (mL) is the volume of the phosphate solution.

2.5. Desorption and regeneration

Batch experiments were performed to probe the recycle times and regeneration methods of the adsorbents [19]. Different types and concentrations of the adsorbent were selected for the regeneration, and the most appropriate type and concentration were determined through a series of experiments. The cyclic process of the adsorbent was studied using the appropriate regenerant as mentioned above, and the optimum adsorption times of $MnFe_2O_4$/MgAl-LDO were also determined.

3. Results and discussion

3.1. Characterization of $MnFe_2O_4$/MgAl-LDO composites

Fig. 2a shows that the surface of hydrotalcite has a typical lamellar structure, which indicated an interlayer space for ion exchange that was suitable for adsorption. Fig. 2b shows that the prepared $MnFe_2O_4$ has a spherical structure and most of the particles have agglomerated together by magnetic force. After the combination of $MnFe_2O_4$ and MgAl-LDO, the lamellar structure of Mg-Al LDO was not destroyed (Fig. 2c). The microstructure of the $MnFe_2O_4$/MgAl-LDO composites was further characterized by TEM, and the results are shown in Fig. 2d. It can be seen that the $MnFe_2O_4$/MgAl-LDO composites have an irregular lamellar structure. In the energy dispersive spectrometer (EDS)

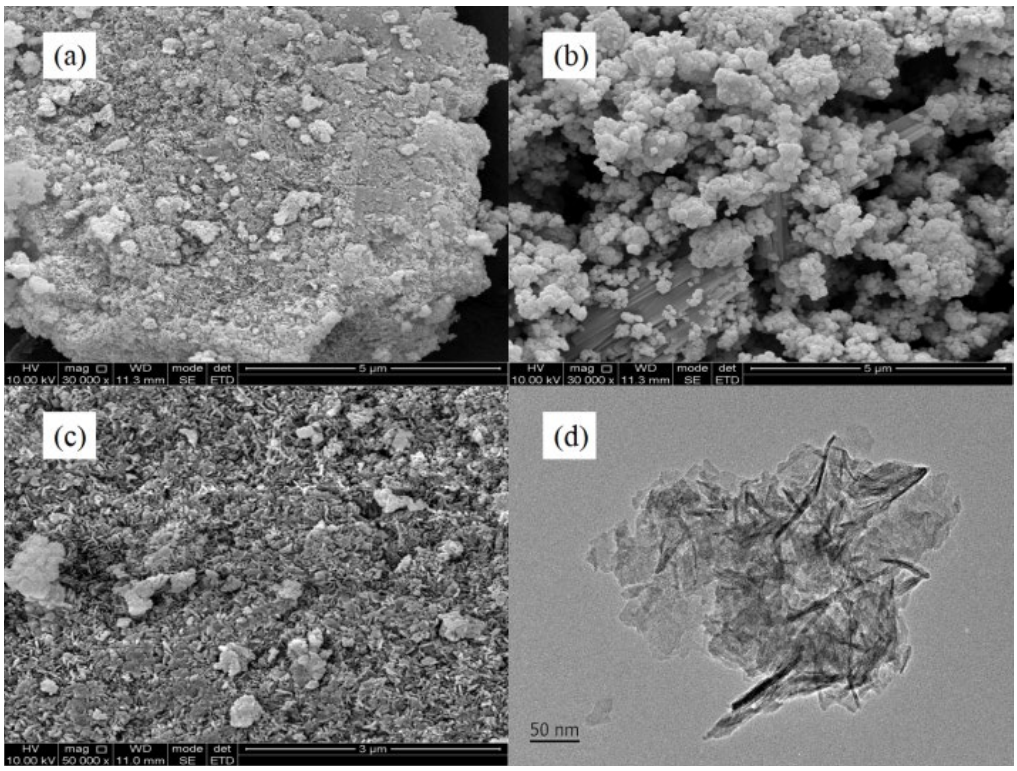

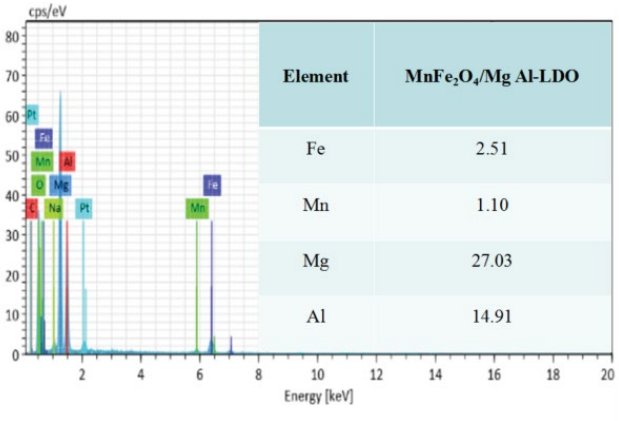

Element	$MnFe_2O_4$/Mg Al-LDO
Fe	2.51
Mn	1.10
Mg	27.03
Al	14.91

Fig. 2. Scanning electron microscope images of (a) MgAl-LDH, (b) $MnFe_2O_4$, (c) $MnFe_2O_4$/MgAl-LDO composites, (d) TEM of $MnFe_2O_4$/MgAl-LDO composites, and (e) EDS image of $MnFe_2O_4$/MgAl-LDO composites.

mapping analysis, the major elements of $MnFe_2O_4$/MgAl-LDO composites are Fe, Mn, Mg, and Al, and the proportions of the elements were observed to be Fe:Mn = 2.28:1 and Mg:Al = 1.81:1, which are in good agreement with the proportions of elements used in the preparation. These results show that the $MnFe_2O_4$/MgAl-LDO composites were prepared successfully.

The X-ray Diffraction (XRD) results of $MnFe_2O_4$ and $MnFe_2O_4$/MgAl-LDO before and after adsorption are shown in Fig. 3a. The characteristic diffraction peaks of $MnFe_2O_4$ at (220), (311), and (440) were observed, which indicated the formation of cubic nanocrystals. Moreover, the narrow and sharp peaks indicated that the samples had a sound structure of regularity and purity [20,21]. There were new characteristic peaks at (003), (018), and (113), which were characteristic of MgAl-LDO, and the peak was sharp compared with that of the standard structure [22,23]. Also, the intensity of the peaks at (003) and (012) had a good multiplier relationship with each other, which indirectly proves that they have a better-layered structure. The $MnFe_2O_4$/MgAl-LDO composites show the XRD patterns of $MnFe_2O_4$ and MgAl-LDO, which suggests the coexistence of both $MnFe_2O_4$ and MgAl-LDO in these composites.

Fig. 3b shows the magnetic hysteresis loops of $MnFe_2O_4$ and $MnFe_2O_4$/MgAl-LDO, which were measured at room temperature. The magnetic induction strength of $MnFe_2O_4$ and $MnFe_2O_4$/MgAl-LDO was 41.525 and 10.978 emu/g, respectively. Owing to the combination of MgAl-LDO and $MnFe_2O_4$, the magnetic saturation strength of the composites was obviously decreased. The coercivity of $MnFe_2O_4$/

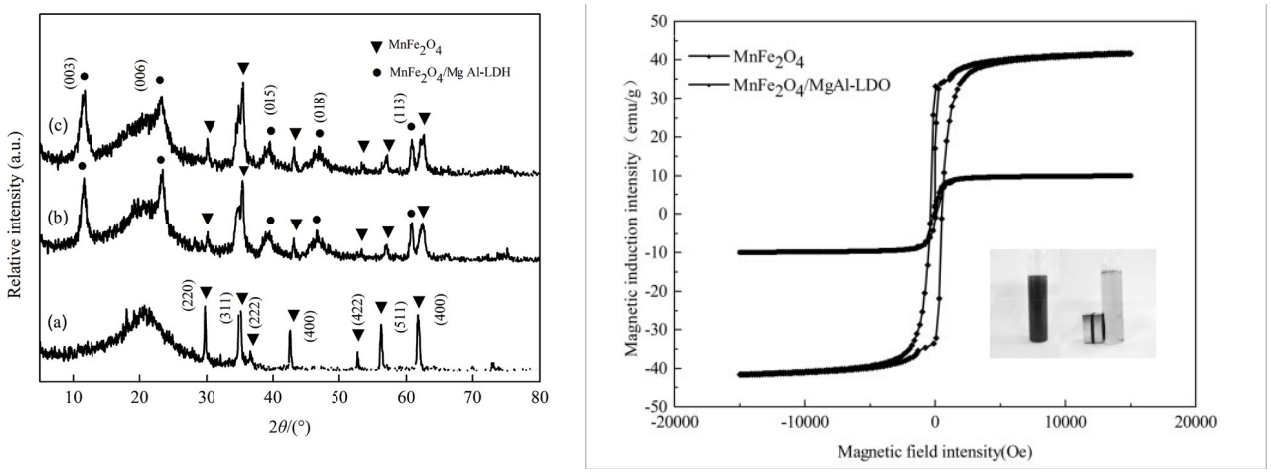

Fig. 3. XRD analysis of (a) $MnFe_2O_4$ and $MnFe_2O_4$/MgAl-LDO composites before and after adsorption and (b) magnetic hysteresis loop of $MnFe_2O_4$ and $MnFe_2O_4$/MgAl-LDO composites.

MgAl-LDO was almost zero, which indicates that it had super-paramagnetic properties. The interpolation in Fig. 3b shows that $MnFe_2O_4$/MgAl-LDO could accumulate around the applied magnetic field in a short time after its rapid dispersion in water. This indicates that the $MnFe_2O_4$/MgAl-LDO still exhibited good magnetism and could be easily separated from an aqueous solution. This characteristic has latent applications in addition to the incomparable advantages of the material over the other conventional adsorbents.

3.2. Effect of adsorbent dosage

The effect of adsorbent dosage on the sorption of phosphate (25 mg/L) was studied by varying the dosage from 0.5 to 5.0 g/L at pH 7. The results are shown in Fig. 4. As can be seen, the adsorption efficiency and adsorption capacity showed an inverse relationship with the dose of $MnFe_2O_4$/MgAl-LDO composites. There was a remarkable increase in the phosphate removal rate when the adsorbent dosage was increased from 0.5 to 5.0 g/L, and the best adsorbent effect was achieved at an adsorbent dosage of 3.0 g/L. This enhancement was ascribed to the increase in the number of adsorption sites for the phosphate in the aqueous solution. Moreover, the large specific surface area of this $MnFe_2O_4$/MgAl-LDO composite has also contributed to this performance. It is known that the addition of magnetic $MnFe_2O_4$/MgAl-LDO adsorbent has a positive influence on the increase in phosphate removal rate when the dosage of the adsorbent is increased gradually. As the adsorption sites were occupied, the adsorption capacity was saturated, which is indicated by the downward trend. Therefore, 3.0 g/L was determined to be the optimum dosage of the magnetic adsorbent in the subsequent experiments.

3.3. Effect of pH

As a momentous single factor, the pH of the solution plays a significant role in the adsorption experiments because of its influence on the reaction system and the exchange of charges and ions on the surface [24]. Here, 3.0 g/L adsorbent was added to 20 mL of phosphate solution with a concentration of 25 mg/L, and the adjustment of pH was accomplished by

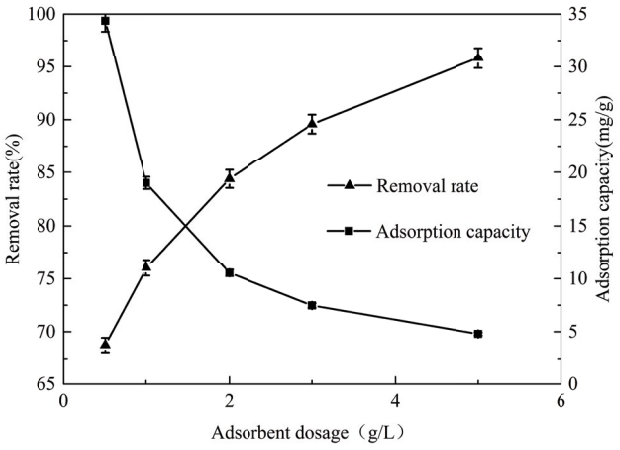

Fig. 4. Removal efficiency and adsorption capacity at different dosages of magnetic adsorbents.

varying the concentrations of the NaOH and HCl solutions. The single factor experiment was performed in a shaker for 240 min at a rotating speed of 170 rpm, and the temperature was 30°C. Fig.5 illustrates the phosphate removal rate and zeta potential of the magnetic adsorbents at different values of pH for the initial solution, which ranged from 2 to 10. The figure shows that the change of pH had an effect on the phosphate removal rate; nevertheless, the phosphate removal rate was above 67.5% on the whole, and the maximum rate was 87.50% at pH = 4. Although the removal rate declined when the pH was >6, but it remained about 80%, which indicated a good adsorption effect that does not depend on the pH of the water environment. Simultaneously, the experiment also showed that the adsorbent had a favorable effect in a near-neutral aqueous solution, which has an important practical significance.

According to the interpolation shown in Fig.5, the zeta potential of the adsorbent clearly decreased with an increase of pH, and the isoelectric point pH_{IEP} was observed to be 8.3. A considerable amount of hydrogen ion is present in the solution when the pH is in the range of 2–6. Owing

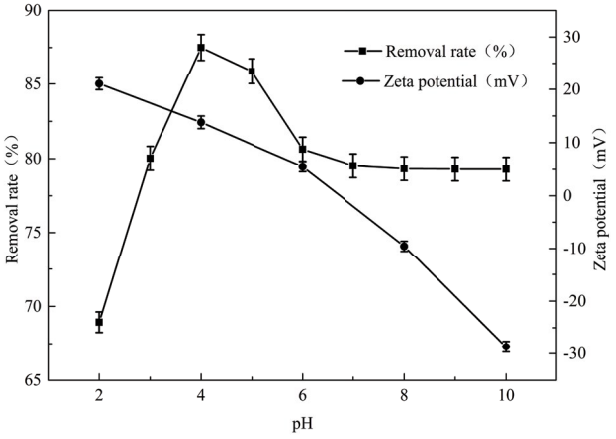

Fig. 5. Removal efficiency of magnetic adsorbent at different initial pH and different Zeta potential.

to the presence of a large number of hydroxyl ions on the surface of hydrotalcite when at pH < 4, a large number of hydrogen ion dominated the protonation in the solution of $MnFe_2O_4$/MgAl-LDO, which contained numerous positive charges [25]. The surface (or laminates) of the magnetic adsorbent was positively charged to adsorb large amounts of phosphate through Coulomb attraction when the pH was lower than 4. The dephosphorization was gradually enhanced with the increase in the pH value of the solution, and the positive charge on the adsorbent surface decreased gradually. However, when pH > 8.3, the negative charges accumulate on the surface of the adsorbent and the electrostatic repulsion between the adsorbent and PO_4^{3-} weakens the adsorption effect [19]. Considering the practical applications, pH = 4 will be adopted in the subsequent adsorption experiments.

3.4. Adsorption kinetics

Experiments on adsorption kinetics were performed with three independent groups of phosphate solutions with different initial concentrations, namely 15, 25, and 35 mg/L, and different contact times ranging from 10 to 480 min. During the initial stage, the adsorption capacity of the magnetic adsorbents increased rapidly with an obvious slope, as shown in Fig. 6a. This is the reason why this adsorbent provided numerous sites for phosphate attachment and change in concentration gradient [23]. After the adsorption test was conducted for 300 min, the process reached its equilibrium due to the presence of a repulsion force and the exchange equilibrium between the phosphate in the solution and the adsorbent surface.

To reveal and explain the mechanism and kinetics involved in the adsorption process, a pseudo-first-order equation and a pseudo-second-order equation were employed to fit the experimental data [26,27]. These equations were classical adsorption description equations based on the adsorption capacity and are given as follows:

$$\ln(q_e - q_t) = q_e - k_1 t \tag{5}$$

$$\frac{t}{q_t} = \frac{1}{k_2 q_e^2} + \frac{t}{q_e} \tag{6}$$

where q_t (mg/g) and q_e (mg/g) are the quantities of phosphate adsorbed on the magnetic adsorbent at t time (min) and counterpoise, respectively. Meanwhile, k_1 (1/min) and k_2 (mg/(g min)) are the rate constants affiliated to the above two equations. The fitting parameters of the kinetic equation are listed in Table 1. From the outcomes of the correlation coefficient (R^2) of the dynamic fitting (Fig. 6b and c), it can be seen that the R^2 of the pseudo-second-order equation was better than that of the pseudo-first-order equation, and it has a better approximation to $R^2 = 1$. The results show that the pseudo-second-order equation model is more practicable for expounding the phosphate adsorption by magnetic $MnFe_2O_4$/MgAl-LDO from aqueous solution. The model has a good fitting effect, which indicates that there may be chemical adsorption and association of chemical bonds between the adsorption sites and phosphate in the adsorption process [28,29].

3.5. Adsorption isotherms

The adsorption thermodynamics experiment is an effective means to investigate the adsorption mechanism. To explore the thermodynamic behavior of the magnetic adsorbents, phosphate solutions with concentrations ranging from 5 to 25 mg/L were measured at 20°C, 30°C, and 40°C, and the removal efficiency and adsorption capacity are shown in Figs. 7a and b, respectively. The results show that the increase in temperature has a positive effect on the adsorption process. The adsorption capacity of the magnetic adsorbent was enhanced from 6.77 to 12.21 mg/g when the temperature was increased, as shown by the column diagram. Nevertheless, the phosphate removal rate decreased slightly from 64% to 53% at the three different temperatures. A high temperature provides more thermal energy for magnetic $MnFe_2O_4$/MgAl-LDO adsorbents and improves their activity; this is an important reason for the increase in the adsorption capacity. Moreover, the isothermal adsorption experiment showed that the adsorption process is an endothermic reaction.

Adsorption models play an essential role in evaluating the adsorption process and determining the relationship between the phosphate ions and adsorption sites. The Langmuir and Freundlich models, which are the commonly used adsorption models, were employed in the isothermal adsorption experiment to investigate the parameters at adsorption equilibrium. The Eqs. (7) and (8) are as follows:

$$\frac{C_e}{q_e} = \frac{C_e}{q_{\max}} + \frac{1}{q_{\max} K_L} \tag{7}$$

$$\ln q_e = \ln K_F + \frac{1}{n} \ln C_e \tag{8}$$

where C_e (mg/L) is the equilibrium concentration of the phosphate solution, q_e is the adsorption capacity (mg/g) of $MnFe_2O_4$/MgAl-LDO at adsorption equilibrium, $q_{\max}$ (mg/g) is the saturated adsorption capacity, and K_L, K_F is the

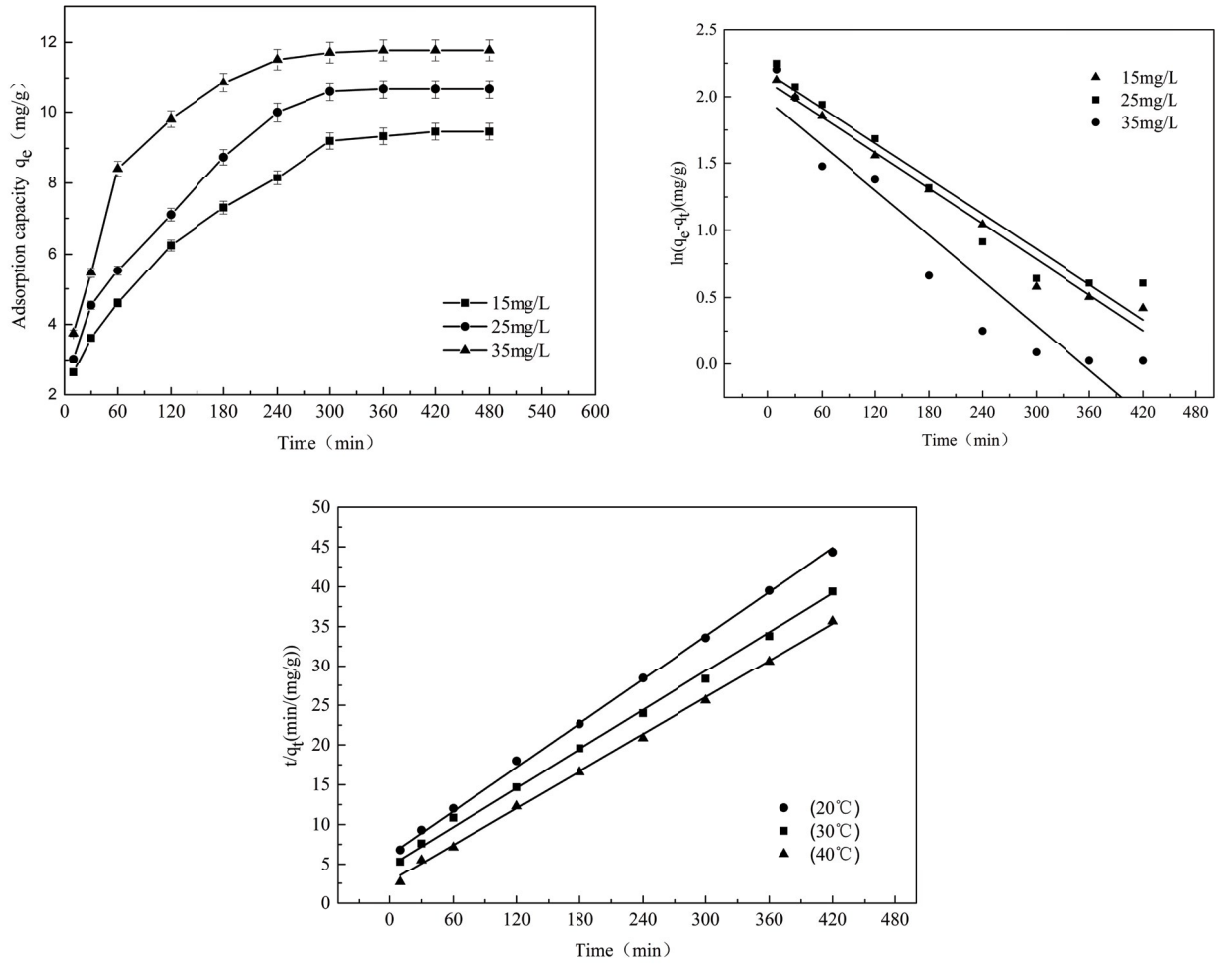

Fig. 6. (a) Adsorption capacity at different adsorption times, (b) pseudo-first-order equation fitting with a straight line, and (c) pseudo-second-order equation fitting with a straight line.

Table 1
Fitting parameters of pseudo-first-order equation and pseudo-second-order equation

Concentration (mg/L)	Pseudo-first-order equation			Pseudo-second-order equation		
	k_1	q_e	R^2	k_2	q_e	R^2
15	0.00442	2.11066	0.97591	0.001279	10.99626	0.99919
25	0.0043	2.17655	0.94041	0.001257	12.49375	0.99748
35	0.00561	1.97202	0.88998	0.002442	12.79918	0.99853

coefficients of Langmuir and Freundlich adsorption models, respectively.

The calculated results of the fitting parameters of the two models are shown in Figs. 7c, d and Table 2. The correlation coefficient (R^2) of the Langmuir isotherm was closer to 1 compared to that of the Freundlich isotherm. This indicates that the Langmuir model is more suitable for describing the phosphate adsorption by magnetic $MnFe_2O_4$/MgAl-LDO adsorbents. The fitting results of this classical model show that the phosphate adsorption by the adsorbent occurs at specific homogeneous reactive sites, and it may be a single layer adsorption process [23,30]. Furthermore, the excellent adsorption efficiency of the adsorbent is closely related to its large specific surface area.

R_L, which is a dimensionless constant, is an important parameter. It indicates whether the adsorption behavior is unfavorable ($R_L > 1$), favorable ($0 < R_L < 1$), linear ($R_L = 1$), or irreversible ($R_L = 0$) [31,32]. It is often employed to determine whether the material is suitable for adsorbing, and the Eq. (9) is as follows:

$$R_L = \frac{1}{1+bC_0} \tag{9}$$

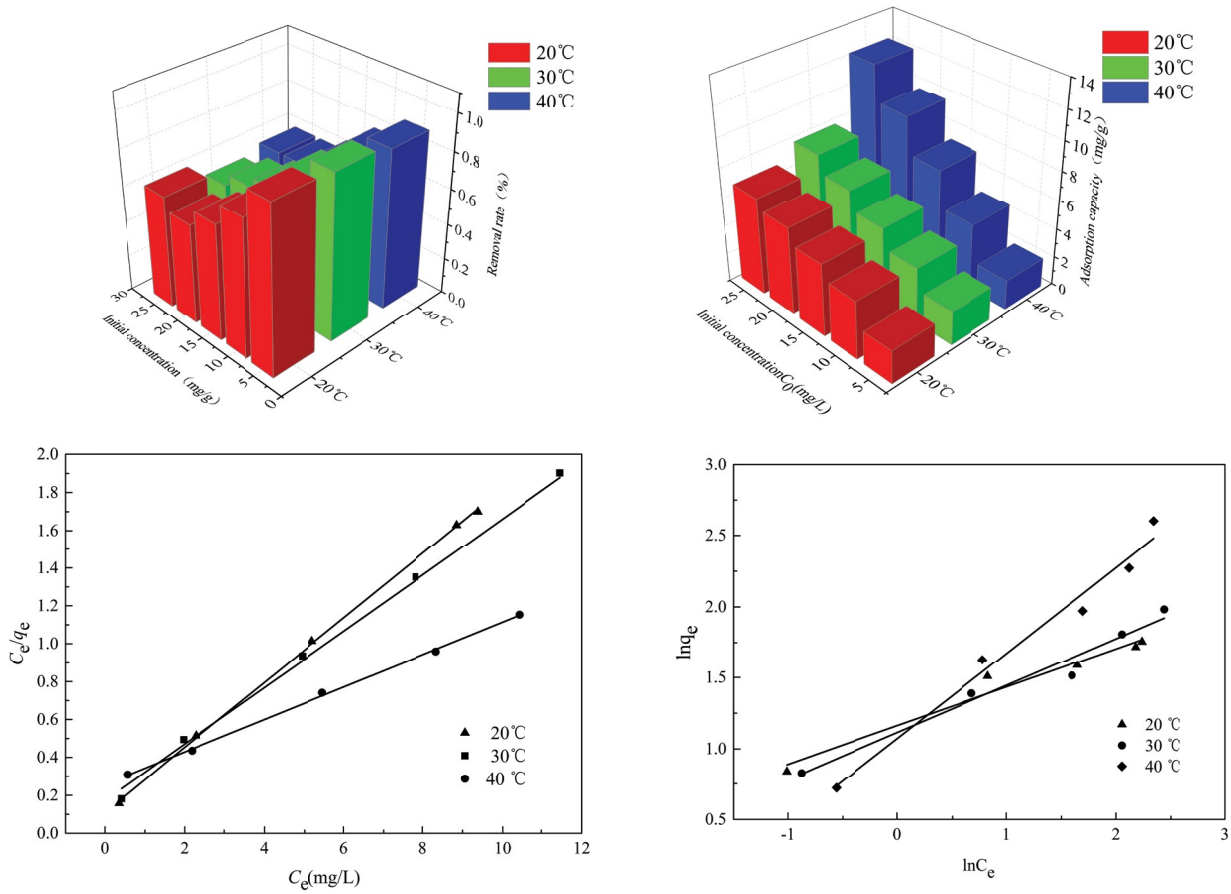

Fig. 7. (a and b) Removal efficiency and adsorption capacity at different reaction temperatures, (c and d) fitting curves of Langmuir and Freundlich isotherm at different temperatures.

Table 2
Fitting parameters of Langmuir and Freundlich isothermal equations at different temperatures

T (°C)	Langmuir isotherm			Freundlich isotherm		
	K_L	q_{max}	R^2	lnK_F	1/n	R^2
20	1.023	6.0745	0.9971	1.1625	3.635	0.9540
30	0.8629	6.7190	0.9936	1.1139	3.022	0.9613
40	0.3338	11.667	0.9994	1.0706	1.662	0.9727

where C_0 is the initial phosphate concentration (mg/L). From the calculated results, it can be seen that the R_L value of magnetic $MnFe_2O_4$/MgAl-LDO is between 0 and 1, indicating that its adsorption of phosphate is favorable.

3.6. Adsorption thermodynamics

Thermodynamics is often used to analyze the changes in energy during the adsorption process, the degree of disorder in the reaction system, and the direction of the reaction process [33]. The results of enthalpy change (ΔH), entropy change (ΔS), and Gibbs free energy (ΔG) can be obtained by borrowing the previous data. The Eqs. (10)–(12) are as follows:

$$\Delta G = -RT\ln K_0 \tag{10}$$

$$\ln K_0 = \frac{\Delta S}{R} - \frac{\Delta H}{RT} \tag{11}$$

$$\Delta G = \Delta H - T\Delta S \tag{12}$$

where ΔG is the Gibbs free energy (kJ/mol), ΔH is the adsorption enthalpy (kJ/mol), ΔS is the adsorption entropy (J/(mol K)), K_0 is the solid–liquid partition coefficient, T is the absolute temperature (K), and R is the ideal gas constant (8.314J/(mol K)). The calculation parameters are shown in Table 3.

The figure of ΔH is positive while the figure of ΔG is negative, which indicates that the adsorption of phosphate by the magnetic adsorbents is an endothermic and spontaneous process. The value of ΔG decreased from −13.845 to −14.961, when the temperature increased from 235.15 to 313.15 K, which indicates that the adsorption of phosphate was enhanced with the increase in external temperature. The entropy change $\Delta S > 0$ revealed that the adsorption of phosphate was a process of increasing entropy and increasing orderliness.

A series of data on the phosphate adsorption capacity of different adsorbents can be found in Table 4. Compared with

Table 3
Thermodynamic parameters of phosphate adsorption by $MnFe_2O_4$/MgAl-LDH

Temperature/*K*	ΔG/(kJ mol^{-1})	ΔH/(kJ mol^{-1})	ΔS/(J (mol K)$^{-1}$)
293.15	–13.845		
303.15	–14.402	2.942	0.556
313.15	–14.961		

Table 4
Comparison of adsorption capacity of phosphates by different adsorbents

Adsorbent	(mg/g)	Refs.
Lanthanum (III) loaded granular ceramic	1.0476	[34]
Calcinated dolomite	0.53	[35]
Coir pith carbon activated by $ZnCl_2$	5.10	[36]
Water treatment residuals	8.20	[37]
$MnFe_2O_4$/MgAl-LDO	34.40	This work

other adsorbents, magnetic $MnFe_2O_4$/MgAl-LDO has a larger adsorption capacity. As the magnetism of the material is beneficial for cyclic utilization, this adsorbent has profound practical application significance.

3.7. Competitive adsorption experiment

In general, water contains diverse anions. It is necessary to explore the adsorption characteristics of the magnetic adsorbents for phosphate and the competitive effect by other anions. Four common anions, CO_3^{2-}, SO_4^{2-}, Cl^-, and NO_3^- were employed in the study, and the concentration of the anions was 20–100 mg/L. In the experiment, 3.0 g/L adsorbent was added to the conical flask containing phosphates and different competitive anions. The concentration of the phosphate solution was 25 mg/L, and the pH was adjusted to be 4. The adsorption process was conducted for 4 h at 30°C. The removal rate of phosphate in the presence of different anions is shown in Fig. 8.

The presence of different anions affects the adsorption of phosphate by $MnFe_2O_4$/MgAl-LDO, and it was found to be different for different ion types and concentrations. Carbonate had the most significant influence, and the removal rate decreased to 73.55% when its concentration was 100 mg/L. The lowest removal rate of phosphate was 76.32% in the presence of sulfate. The effects of nitrate and chloride on this process are relatively weak, compared with those of the other two divalent anions. The effect of carbonate was greater than that of the other three anions at the same concentration, and with the increase in concentration, the removal rate of phosphate decreased. However, the minimum removal rate was still more than 70%, and the order of the influence strength was as follows: $CO_3^{2-} > SO_4^{2-} > Cl^- > NO_3^-$. Carbonate had an obvious influence on the adsorption process because of its ability to participate in the structural reorganization of Mg-Al hydrotalcite, and this was the reason for the high charge number. At the same time, the inner complexes formed by carbonate and sulfate with the hydroxyl

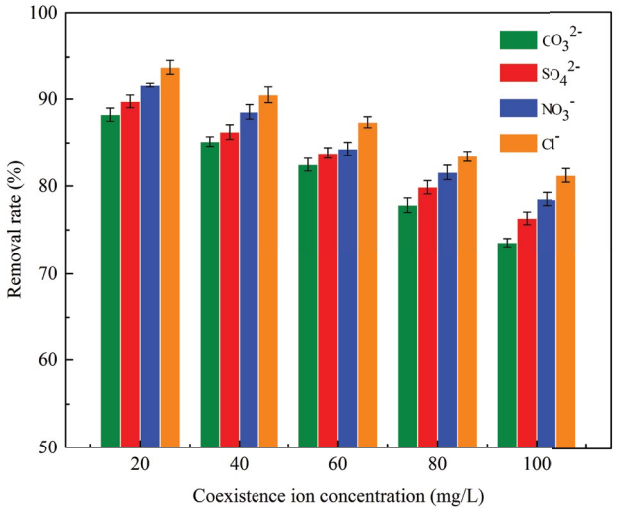

Fig. 8. Competitive adsorption experiments for phosphate with CO_3^{2-}, SO_4^{2-}, Cl^-, and NO_3^-.

groups on the adsorbent may also have promoted this process (chloride and nitrate can only form outer complexes with hydroxyl groups on this adsorbent) [38,39].

3.8. Desorption and cyclic adsorption times experiment

To study the desorption effect and degree of different desorption materials, 0.1 mol/L NaCl, NaOH, and Na_2CO_3 solutions were used. The magnetic adsorbent adsorbed with phosphate was put into the four desorption solutions in the same amount. The resolving rate was determined after 12 h of reaction in a constant temperature shaker at a certain speed, and the results are shown in Fig. 9a. After Na_2CO_3 was chosen as the regenerant, the adsorbent was regenerated with different concentrations of Na_2CO_3 solution, and its regeneration rate was calculated to determine the optimal concentration of the regenerant. The experimental results are shown in Fig. 9b, it shows that the regeneration rate of the four different regenerants is 89% of the mixed solution of Na_2CO_3 and NaOH, and 32% of the NaCl solution. Considering the convenience and economic benefits of the actual use process, the Na_2CO_3 solution was finally selected, and the regeneration rate was 82%. Carbonate has the function of exchanging between layers. Carbonate can transfer from a high concentration solution to a low concentration solution, that is, to the interlaminar movement of hydrotalcite [40]. The cyclic test results (Fig. 9c) show that the removal rate of $MnFe_2O_4$/MgAl-LDO

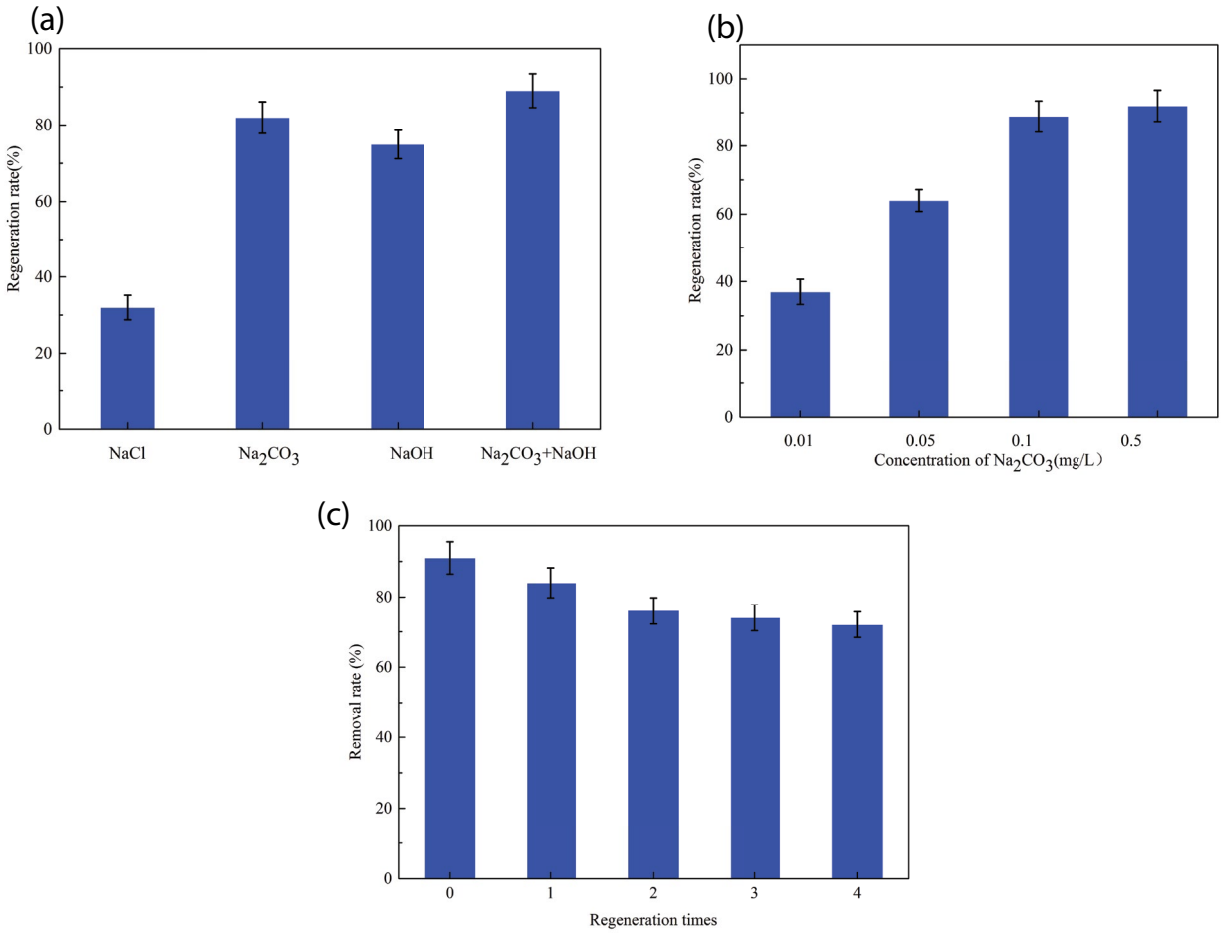

Fig. 9. (a) Desorbent selection, (b) desorption effect of different Na_2CO_3 solution concentrations, and (c) cyclic adsorption effect of $MnFe_2O_4$/MgAl-LDO.

after 0 regeneration was 91% (original adsorbent), and the phosphate removal rates from the first to the fourth regeneration were 85%, 76%, 74%, and 72%, respectively, which indicates that the regenerated adsorbent had a good adsorption effect on phosphate.

3.9. Adsorption mechanism

The clarification of the phosphate adsorption mechanism is of great significance for further analysis of material properties and their practical applications. Zeta potential detection and FTIR analysis were applied for explicating the mechanism of phosphate adsorption by magnetic $MnFe_2O_4$/MgAl-LDO, and the schematic is shown in Fig. 10. The isoelectric point's pH_{IEP} of the magnetic adsorbents before and after adsorption was observed to be 8.3 and 5.4, respectively, and it can be seen that the isoelectric points declined significantly. Phosphoric acid has the characteristics of gradual dissociation. The dissociation equilibrium Eq. (13) is as follows:

$$H_3PO_4 \xleftrightarrow{K_1} H_2PO_4^{2-} + H^+ \xleftrightarrow{K_2} HPO_4^{2-} + 2H^+ \overset{K_3}{\leftrightarrow} PO_4^{3-} + 3H^+ \quad (13)$$

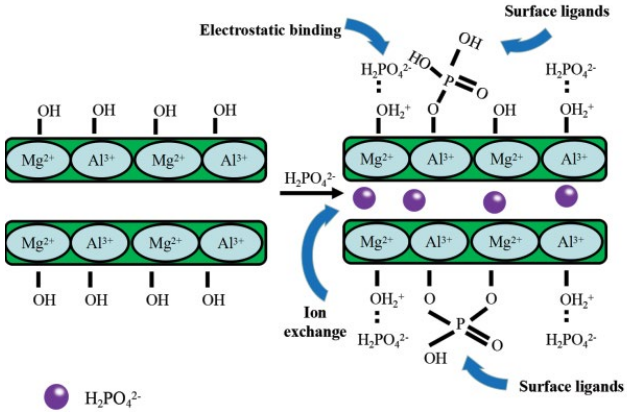

Fig. 10. Schematic illustration of phosphate adsorption by $MnFe_2O_4$/MgAl-LDO.

where $pKa_1 = 2.12$, $pKa_2 = 7.21$, and $pKa_3 = 12.67$ [41]. The dissociation process of phosphate can be promoted or inhibited by the change in the pH of the solution. Moreover, its change influences the surface charge of the adsorbent. When the pH of the solution was lower than the pH_{IEP} of $MnFe_2O_4$/MgAl-LDO, the hydroxyl on the surface of the adsorbent combined

with hydrogen ions in the solution and was converted into OH_2^+. This process promoted the binding of phosphates with the protonated hydroxyl groups. The lower pH also was conducive to the exchange of $H_2PO_4^{2-}$ with CO_3^{2-} interlayer ions, which is also an indispensable process for the removal of phosphate [23]. The increase in the pH of the solution led to a decrease in protons in the solution. Negative charges accumulated on the adsorbent surface when the pH exceeded the isoelectric point. The surface of the adsorbent exhibited electronegativity, and the electrostatic repulsion of hydroxyl and phosphate hindered its electrostatic binding. This process also weakened the exchange of PO_4^{3-} with the interlayer anion CO_3^{2-}. Phosphates existed as the form of PO_4^{3-}, as they were completely dissociated when the dissociation constant was $pKa_3 = 12.67$. These superpositions caused a decrease in the adsorption capacity of magnetic $MnFe_2O_4$/MgAl-LDO for phosphate in alkaline conditions.

The FTIR results can further explain the process of adsorption of phosphate by the adsorbent. The FTIR spectra of LDH, $MnFe_2O_4$/MgAl-LDO before and after the adsorption of phosphates are presented in Fig. 11. The remarkable and intense peaks shown by the spectral lines (b) and (c) at 576 cm^{-1} can be ascribed to the Fe–O stretching vibration of tetrahedral $MnFe_2O_4$ [11]. The spectra peak position of $MnFe_2O_4$ does not change significantly when it is combined with MgAl-LDO. Nevertheless, its peak value decreased, which confirmed that $MnFe_2O_4$ was encapsulated in it once again. The obvious absorption peaks of MgAl-LDO appear in the FTIR spectra. The absorption peak at 3,450 cm^{-1} was attributed to the stretching vibration of the O-H bonds on the surface of the layer and the interlayer water molecules [42]. The additional absorption peak near 1,370 cm^{-1} was ascribed to the antisymmetric stretching vibration of the C–O bond, which indicates the existence of CO_3^{2-} in the interlayer of MgAl-LDH [43]. It can be seen from the comparison of the spectrum line in the graph that the peaks in MgAl-LDH are also reflected in the spectral lines of $MnFe_2O_4$/MgAl-LDO, and they are consistent. However, the characteristic absorption peaks in the spectra indicated by (b) and (c) were weakened than that in the spectrum indicated by (a), which indicates that some CO_3^{2-} of the interlayer dissipated in the form of water molecules and carbon dioxide during the calcination process [11,44].

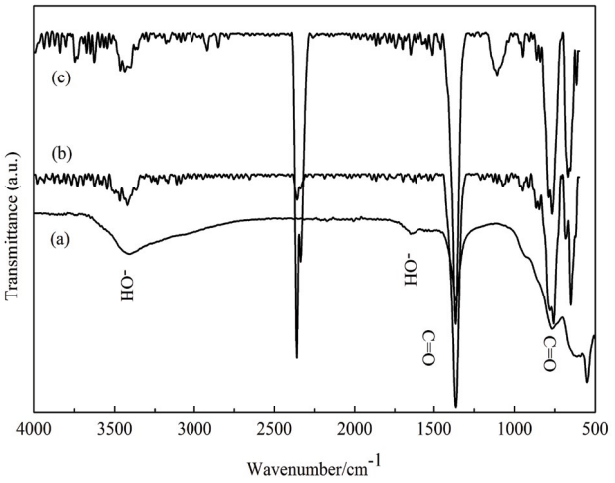

Fig. 11. (a) FTIR image of $MnFe_2O_4$, $MnFe_2O_4$/MgAl-LDO, (b) before, and (c) after adsorption.

The characteristic absorption peaks of Mg–Al hydrotalcite at 630 cm^{-1} still existed, but the intensity of the peaks decreased, indicating that metal bonds were involved in the adsorption process of phosphate [28]. The strong antisymmetric vibration peaks of P–O at 1,053 cm^{-1} indicate that phosphate was adsorbed by the metal bonds on the surface of hydrotalcite and may be combined in the form of monodentate ligand or bidentate ligand [9]. The complex Eqs. (14)–(17) of phosphate with metal hydroxides are as follows [19]:

$$\equiv MeOH + PO_4^{3-} = \equiv MePO_4^{2-} + OH^- \quad (14)$$

$$2 \equiv MeOH + PO_4^{3-} = (\equiv Me)_2 PO_4^- + 2OH^- \quad (15)$$

$$\equiv MeOH + HPO_4^{2-} = \equiv MeHPO_4^- + OH^- = \equiv MePO_4^{2-} + H_2O \quad (16)$$

$$\equiv MeOH + H_2PO_4^- = \equiv MeH_2PO_4 + OH^- = \equiv MeHPO_4^- + H_2O \quad (17)$$

The increase in the pH of the solution after adsorption also indicates the occurrence of a coordination process, and it shows that the hydroxyl groups on the surface of $MnFe_2O_4$/MgAl-LDO also played an important role in the phosphate adsorption process. Based on the analysis and hypothesis mentioned above, the process of phosphate adsorption by magnetic adsorbents should be attributed to: (1) the adsorption of hydroxyl groups on the surface of the adsorbents after protonation; (2) the ion exchange between phosphate and interlayer CO_3^{2-}; and (3) the coordination between phosphate and hydroxyl groups on the surface of adsorbents.

4. Conclusions

In this study, magnetic $MnFe_2O_4$/MgAl-LDO was prepared by the co-precipitation method, and it showed good adsorption effect on phosphate at pH = 4; the optimum adsorption time was 3 h and the reaction temperature was 30°C. The optimum dosage was 3 g/L, and the maximum adsorption capacity was 34.4 mg/g. The adsorption equilibrium of phosphate was achieved after 300 min, and the pseudo-second-order equation model was well fitted to the adsorption kinetic process. The results of adsorption thermodynamics show that the adsorption of phosphate by the adsorbent is a spontaneous and endothermic process and that the degree of freedom is increased. The phosphate removal rate of $MnFe_2O_4$/MgAl-LDO exceeded 85%, and it is easy to regenerate and recycle.

Acknowledgements

We thank the editors and reviewers for their helpful suggestions on this paper. This project was supported in part by the National Natural Science Fund (41263010), Inner

Mongolia University of Science and Technology Innovation Fund (2016QDL-B08), and Scientific Research Projects of University in Inner Mongolia (NJZY19132).

References

[1] H.W. Paerl, Controlling eutrophication along the freshwater–marine continuum: dual nutrient (N and P) reductions are essential, Estuaries Coasts, 32 (2009) 593–601.

[2] Y. Jiang, Z. Nan, S. Yang, Risk assessment of water quality using monte carlo simulation and artificial neural network method, J. Environ. Manage., 122 (2013) 130–136.

[3] Z. Ju, Z. Yu, H. Deng, Effects of aquatic vegetation rehabilitation on phosphorus in water and sediments of urban landscape waters, J. Lake Sci., 27 (2015) 234–242.

[4] M. Garrett, J. Wolny, E. Truby, C. Heil, C. Kovach, Harmful algal bloom species and phosphate-processing effluent: field and laboratory studies, Mar. Pollut. Bull., 62 (2011) 596–601.

[5] D. Wang, N. Chen, Y. Yu, Investigation on the adsorption of phosphorus by Fe-loaded ceramic adsorbent, J. Colloid Interface Sci., 464 (2016) 277–284.

[6] P. Chutia, S. Kato, T. Kojima, S. Satokawa, Adsorption of As(v) on surfactant-modified natural zeolites, J. Hazard. Mater., 162 (2009) 204–211.

[7] M. Barr, E.S. Arnista, Adsorption studies on clays I. The adsorption of two alkaloids by activated attapulgite, halloysite, and kaolin, J. Pharm. Sci., 46 (1957) 486–489.

[8] E. Bulut, M. Zacar, A. Engil, Equilibrium, and kinetic data and process design for adsorption of congo red onto bentonite, J. Hazard. Mater., 154 (2008) 613–622.

[9] K. Yang, L. Yan, Y. Yang, S. Yu, R. Shan, H. Yu, Adsorptive removal of phosphate by Mg–Al, and Zn–Al layered double hydroxides: kinetics, isotherms and mechanisms, Sep. Purif. Technol., 124 (2014) 36–42.

[10] C. Liu, M. Zhang, G. Pan, Efficiency and mechanism of phosphate removal by ultrathin layered double hydroxide nanosheets, J. Chin. Environ. Eng., 12 (2018) 2446–2456.

[11] L. Lv, J. He, M. Wei, D.G. Evans, X. Duan, Uptake of chloride ion from aqueous solution by calcined layered double hydroxides: equilibrium and kinetic studies, Water Res., 40 (2006) 735–743.

[12] M. Liao, W. Zhu, C. Han, On the preparation of MgAl-LDH and its adsorption properties for chromium (VI), J. Saf. Environ., 16 (2016) 200–207.

[13] L. Deng, Z. Shi, X. Peng, S. Zhou, Magnetic calcinated cobalt ferrite/magnesium aluminum hydrotalcite composite for enhanced adsorption of methyl orange, J. Alloys Compd., 688 (2016) 101–112.

[14] Y. Guo, X. Yue, J. Liu, Adsorption of fluoride ion by calcined Mg/Al/Fe hydrotalcite, J. Chin. Environ. Eng., 9 (2015) 5921–5926.

[15] U. Lamdab, K. Wetchakun, W. Kangwansupamonkon, N. Wetchakun, Effect of a pH-controlled co-precipitation process on rhodamine B adsorption of $MnFe_2O_4$ nanoparticles, RSC Adv., 8 (2018) 6709–6719.

[16] S.M. Vargas, Martínez, A.I. Mernández, E.E. Hernandez, As(III) and As(v) adsorption on manganese ferrite nanoparticles, J. Mol. Struct., 1154 (2017) 524–534.

[17] C. Yi, C. Hang, L. Yang, Adsorption of chromium (VI) by nano-manganese ferrite, Bull. Chin. Ceram. Soc., 36 (2017) 2900–2906.

[18] T. Jin, X. Zhang, J. Xu, Preparation of manganese ferrite/humic acid composite and its adsorption properties for methylene blue, J. Chin. Appl. Chem., 33 (2016) 336–342.

[19] X. Cheng, Phosphorus Recovery from Sewage Water by Layered Double Hydroxides as an Adsorbent by Vivianite Precipitation, Harbin Institute of Technology, Harbin, China, 2010.

[20] S. Lv, X. Chen, Y. Ye, S. Yin, J. Cheng, M. Xia, Rice hull/$MnFe_2O_4$ composite: preparation, characterization and its rapid microwave-assisted COD removal for organic wastewater, J. Hazard. Mater., 171 (2009) 634–639.

[21] S. Zhang, H. Niu, Y. Cai, X. Zhao, Y. Shi, Arsenite and arsenate adsorption on coprecipitated bimetal oxide magnetic nanomaterials: $MnFe_2O_4$ and $CoFe_2O_4$, Chem. Eng. J., 158 (2010) 599–607.

[22] M.P. Reddy, A.M.A. Mohamed, X.B. Zhou, A facile hydrothermal synthesis, characterization and magnetic properties of mesoporous $CoFe_2O_4$ nanospheres, J. Magn. Magn. Mater., 388 (2015) 40–44.

[23] L. Deng, Z. Shi, X. Peng, L. Wang, Adsorption of phosphate in aqueous phase using magnetic $CoFe_2O_4$/MgAl-LDH, J. Chin. Environ. Eng., 10 (2016) 586–592.

[24] J. Das, B.S. Patra, N. Baliarsingh, K.M. Parida, Adsorption of phosphate by layered double hydroxides in aqueous solutions, Appl. Clay Sci., 32 (2006) 252–260.

[25] Y. Yang, N. Gao, W. Chu, Y. Zhang, Y. Ma, Adsorption of perchlorate from aqueous solution by the calcination product of Mg/(Al-Fe) hydrotalcite-like compounds, J. Hazard. Mater., 209–210 (2012) 318–325.

[26] X. Cheng, X. Huang, X. Wang, B. Zhao, A. Chen, D. Sun, Phosphate adsorption from sewage sludge filtrate using zinc-aluminum layered double hydroxides, J. Hazard. Mater., 169 (2009) 958–964.

[27] P. Cai, H. Zheng, C. Wang, H. Ma, J. Hu, Y. Pu, Competitive adsorption characteristics of fluoride and phosphate on calcined Mg–Al–CO_3 layered double hydroxides, J. Hazard. Mater., 213–214 (2012) 100–108.

[28] R. Li, J. Wang, B. Zhou, M.K. Awasthi, A. Ali, Z. Zhang, Enhancing phosphate adsorption by Mg/Al layered double hydroxide functionalized biochar with different Mg/Al ratios, Sci. Total Environ., 559 (2016) 121–129.

[29] L. Yan, K. Yang, R Shan, T. Yan, J. Wei, Kinetic, isotherm and thermodynamic investigations of phosphate adsorption onto core-shell Fe_3O_4@LDHs composites with easy magnetic separation assistance, J. Colloid Interface Sci., 448 (2015) 508–516.

[30] R. Shan, L. Yan, K. Yang, S. Yu, Y. Hao, Magnetic Fe_3O_4/MgAl-LDH composite for effective removal of three red dyes from aqueous solution, Chem. Eng. J., 252 (2014) 38–46.

[31] Y. Li, B. Gao, T. Wu, D. Sun, X. Li, Hexavalent chromium removal from aqueous solution by adsorption on aluminum-magnesium mixed hydroxide, Water Res., 43 (2009) 3067 –3075.

[32] X. Zhang, C. Jiao, J. Wang, Q. Liu, R. Li, Removal of uranium(VI) from aqueous solutions by magnetic schiff base: kinetic and thermodynamic investigation, Chem. Eng. J., 198–199 (2012) 412–419.

[33] X. Yuan, Y. Wang, J. Wang, C. Zhou, Q. Tang, X. Rao, Calcined graphene/MgAl-layered double hydroxides for enhanced Cr(VI) removal, Chem. Eng. J., 221 (2013) 204–213.

[34] N. Chen, C. Feng, Z. Zhang, R., Y. Gao, Preparation and characterization of lanthanum (III) loaded granular ceramic for phosphorus adsorption from aqueous solution, J. Taiwan Inst. Chem. Eng., 43 (2012) 783–789.

[35] S. Karaca, A. Gürses, M. Ejder, Adsorptive removal of phosphate from aqueous solutions using raw and calcinated dolomite, J. Hazard. Mater., 128 (2006) 273–279.

[36] C. Namasivayam, D. Sangeetha, Equilibrium and kinetic studies of adsorption of phosphate onto $ZnCl_2$ activated coir pith carbon, J. Colloid Interface Sci., 280 (2004) 359–365.

[37] L. Bai, C. Wang, L. He, Y. Pei, Influence of the inherent properties of drinking water treatment residuals on their phosphorus adsorption capacities, J. Environ. Sci., 26 (2014) 2397–2405.

[38] G. Lefèvre, In situ Fourier-transform infrared spectroscopy studies of inorganic ions adsorption on metal oxides and hydroxides, Adv. Colloid Interface Sci., 107 (2004) 109–123.

[39] J. Lǔ, H. Liu, R. Liu, X. Zhao, L. Sun, J. Qu, Adsorptive removal of phosphate by a nanostructured Fe–Al–Mn tri-metal oxide adsorbent, Powder Technol., 233 (2013) 146–154.

[40] Y. Wu, Adsorption of Thiocyanate and Fluorine on Calcined Mg/Al Layered Double Hydroxides, Taiyuan University of Technology, Taiyuan, China, 2015, pp. 55–56.

[41] N.I. Chubar, V.A. Kanibolotskyy, V.V. Strelko, G.G. Gallios, V.F. Samanidou, T.O. Shaposhnikova, Adsorption of phosphate ions on novel inorganic ion exchangers, Colloids Surf., A, 255 (2005) 55–63.

[42] R. Extremera, I. Pavlovic, M.R. Pérez, C. Barriga, Removal of acid orange 10 by calcined Mg/Al layered double hydroxides

from water and recovery of the adsorbed dye, Chem. Eng. J., 213 (2012) 392–400.
[43] R.M.M. Dos Santos, R.G.L. Goncalves, V.R.L. Constantino, Removal of acid green 68:1 from aqueous solutions by calcined and uncalcined layered double hydroxides, Appl. Clay Sci., 80–81 (2013) 189–195.
[44] H. Zaghouane-Boudiaf, M. Boutahala, L. Arab, Removal of methyl orange from aqueous solution by uncalcined and calcined MgNiAl layered double hydroxides (LDHs), Chem. Eng. J., 187 (2012) 142–149.